AD-A172 675 COHERENT SCATTERING OF LIGHT BY NUCLEAR SPINS(U) 1/1
MARYLAND UNIV COLLEGE PARK DEPT OF PHYSICS AND
ASTRONOMY J WEBER 01 JUN 86 AFOSR-TR-86-0908
UNCLASSIFIED F49620-81-C-0024 F/G 20/12 NL

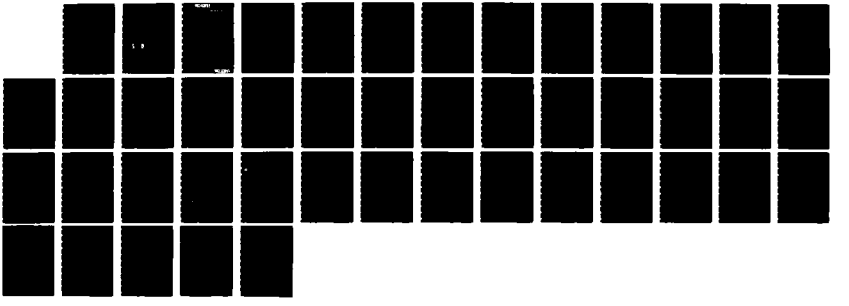

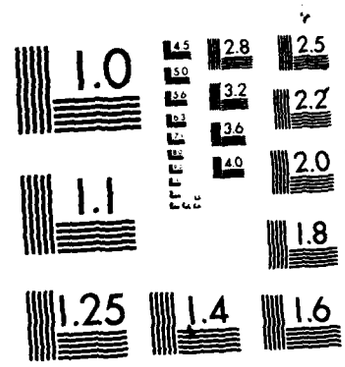

(2)

Coherent Scattering of Light by Nuclear Spins

Final Report

to

Air Force Office of Scientific Research

June 1, 1986

J. Weber

University of Maryland, College Park, Maryland 20742

and

University of California, Irvine, California 92717

UNIVERSITY OF MARYLAND
DEPARTMENT OF PHYSICS AND ASTRONOMY
COLLEGE PARK, MARYLAND

UNCLASSIFIED

SECURITY CLASSIFICATION OF THIS PAGE (When Data Entered)

REPORT DOCUMENTATION PAGE	READ INSTRUCTIONS BEFORE COMPLETING FORM
1. REPORT NUMBER AFOSR-TR- 86-0908	2. GOVT ACCESSION NO. AD-A172 675 — 3. RECIPIENT'S CATALOG NUMBER
4. TITLE (and Subtitle) Coherent Scattering of Light by Nuclear Spins	5. TYPE OF REPORT & PERIOD COVERED Annual Report
	6. PERFORMING ORG. REPORT NUMBER
7. AUTHOR(s) J. Weber	8. CONTRACT OR GRANT NUMBER(s) AFOSR-85-0159
9. PERFORMING ORGANIZATION NAME AND ADDRESS Department of Physics and Astronomy University of Maryland College Park, Maryland 20742	10. PROGRAM ELEMENT, PROJECT, TASK AREA & WORK UNIT NUMBERS 61102F, 2301, A8 N/A
11. CONTROLLING OFFICE NAME AND ADDRESS Air Force Office of Scientific Research Bolling Air Force Base, Washington, D.C. 20332	12. REPORT DATE June 1, 1986
	13. NUMBER OF PAGES 31 + figures
14. MONITORING AGENCY NAME & ADDRESS (if different from Controlling Office) Air Force Office of Scientific Research NP	15. SECURITY CLASS. (of this report) Unclassified
	15a. DECLASSIFICATION/DOWNGRADING SCHEDULE

16. DISTRIBUTION STATEMENT (of this Report)

Approved for public release; distribution unlimited

17. DISTRIBUTION STATEMENT (of the abstract entered in Block 20, if different from Report)

18. SUPPLEMENTARY NOTES

19. KEY WORDS (Continue on reverse side if necessary and identify by block number)

20. ABSTRACT (Continue on reverse side if necessary and identify by block number)

A new kind of coherent interaction is possible for strongly coupled scatterers. The general theory is presented and applied to the coherent absorption of light by an ensemble of coupled nuclei, with polarized spins.

DD FORM 1 JAN 73 1473 EDITION OF 1 NOV 65 IS OBSOLETE

SECURITY CLASSIFICATION OF THIS PAGE (When Data Entered)

UNCLASSIFIED

ABSTRACT

A new kind of coherent interaction is possible for strongly coupled scatterers. The general theory is presented and applied to the coherent absorption of light by an ensemble of coupled nuclei, with polarized spins.

Introduction

The interaction of a beam of particles with large numbers of scatterers is being explored. An earlier paper[1] showed that large increases in transition rates are possible for correlated scatterer states.

Here a new kind of coherent interaction is studied. It is shown that very large increases in total cross section are possible for tightly bound scatterers interacting with certain kinds of radiation.

Three kinds of experiments have been carried out, in which the coupling of scatterers with each other is important. These are:

a) Low energy antineutrinos interacting with nuclei of a solid,

b) Raman scattering of light by electrons in a thin conducting film on the surface of a polarized dielectric, and

c) Interaction of light with polarized nuclei of a crystal

For a) the theory is the interaction of two current densities and the lowes order process is antineutrino scattering, b) is a scattering process described b the interaction of light with electrons, and c) is an absorption process descri by the interaction of light with magnetic moments.

All of these processes may have total cross sections orders greater than the corresponding ones for scatterers which are not tightly bound. This appear true for all tightly bound scatterer interactions. To explore this most import feature in detail, we consider first some examples described by interacting currents. Later the theory of the coherent interaction of light with nuclear moments of a solid will be presented, followed by a description of experiments.

INTERACTION OF FOUR CURRENT DENSITIES

Let us consider the S matrix for interaction of two four current densities[2] given by

$$S = \frac{i}{\hbar c}\int \langle F|\bar{\psi}_S \Gamma \psi_S \bar{\psi}_I K \psi_I|0\rangle \, d^4x \qquad (1)$$

$\langle F|$ is the final state, $|0\rangle$ is the original state. $\bar{\psi}_S$ is a creation operator for scatterer S, $\bar{\psi}_I$ is a creation operator for incident particle I. ψ_S and ψ_I are the corresponding annihilation operators. Γ and K are position independent operators.

The operators $\bar{\psi}_S$ and $\bar{\psi}_I$ are represented by the following expansions.[3]

$$\bar{\psi}_S = \sum_n \sum_j \psi^*_{sjn}(\bar{r}-\bar{r}_n)\, a^\dagger_{jn} \qquad (2A)$$

$$\bar{\psi}_I = \frac{1}{\sqrt{V}} \sum_k \bar{U}_{Ik}\, e^{-\frac{i}{\hbar}\bar{p}_{Ik}\cdot\bar{r}}\, d^\dagger_k \qquad (2B)$$

In (2) $\bar{r}$ is the position three vector, $a^\dagger_{jn}$ is a creation operator for the state with wavefunction ψ^*_{sjn} . n refers to the n^{th} scattering site. $d^\dagger_k$ is a creation operator for an incident particle with known momentum $\bar{p}_{Ik}$ U_{Ik} is an incident particle spinor.

SINGLE SCATTERER ON N SITES

Suppose further that there are N sites in a solid material. For the states ψ_{sjn}, harmonic oscillator states are selected. Consider the case of a single scatterer.

The single scatterer can be prepared in a harmonic oscillator ground state with equal probability to be on any one of the N sites. The original scatterer state for the single scatterer is taken to be

$$\frac{1}{\sqrt{N}} \sum_{n=1}^{n=N} a_{on}^{\dagger} \left| \begin{matrix} \text{VACUUM} \\ \text{STATE} \end{matrix} \right\rangle \tag{3}$$

Let us assume that the scatterer position probability distribution $\psi_{sjn}^{*} \psi_{sjn}$ is not changed by the scattering. Therefore the effect of the scattering can only be a phase shift such that each final scatterer state $(\psi_{sjn})_F$ is related to the original state $(\psi_{sjn})_o$ by

$$(\psi_{sjn})_F = (\psi_{sjn})_o \, e^{i \Delta p_r x^r / \hbar} \tag{4}$$

(4) implies that each component in the momentum decomposition of the scatterer is shifted by the three momentum $\Delta \bar{p}$, corresponding to momentum exchange $\Delta \bar{p}$.

For a harmonic oscillator wavefunction centered at radius vector $\bar{r}_n$,

$$\psi_{sjn} = \left(\frac{\alpha}{\pi}\right)^{3/2} e^{-\alpha^2 |\bar{r} - \bar{r}_n|^2} \tag{5}$$

In (5) α specifies the volume occupied by the particle.

We assume spin zero scatterers, $\Gamma = 1$, (1).(2).(3), and (4) give

$$S = \frac{\bar{U}_{IF} K U_{IO}}{\hbar c V N} \int \left(\frac{\alpha}{\pi}\right)^{3/2} \sum_{n=1}^{n=N} e^{-\alpha|\bar{r}-\bar{r}_n|^2 + \frac{i}{\hbar}(p_{IO}-p_{IF}-\Delta p)_\mu x^\mu} d^4x \tag{6}$$

In (6) p_{IO} and p_{IF} are the original and final 4 momenta of the incident particle, respectively. As $\alpha \to \infty$ (6) becomes

$$S \to \frac{\bar{U}_{IF} K U_{IO}}{\hbar V N} \sum_{n=1}^{n=N} e^{\frac{i}{\hbar}(\bar{p}_{IO}-\bar{p}_{IF}-\Delta\bar{p})\cdot\bar{r}_n} \int e^{\frac{i}{\hbar}(E_{IO}-E_{IF}-\Delta E)t} dt \tag{6A}$$

(6) indicates the possibility of exchanging the entire momentum $\Delta\bar{p}$ at <u>any</u> of the possible N sites at which the single scatterer may be found.

For momentum conservation, the sum in (6) approaches N. The possibilities for exchange of energy and momentum do not appear to severely restrict the solid angle into which an incident particle would be scattered.

COHERENT MOMENTUM TRANSFER PHASE SHIFT INTERACTIONS

Suppose now that we have N tightly bound scatterers. If an incident particle interacts with one scatterer, its strong coupling with all other nuclei might be expected to affect the interaction with an incident particle in a profound way. Consider (6). As already noted, the entire momentum $\Delta\bar{p}$ can be exchanged at any site without possibility of identifying the site of the scattering. With sufficiently strongly coupled particles, momentum transfer at a single site is immediately exchanged with all other particles, with no possibility of identifying the site at which the scattering occurred.

For N tightly bound scatterers, the original state is selected as

$$a_{o1}^{\dagger} a_{o2}^{\dagger} a_{o3}^{\dagger} \cdots a_{oN}^{\dagger} \left| \begin{matrix} \text{VACUUM} \\ \text{STATE} \end{matrix} \right\rangle \qquad (7)$$

For nuclei in a solid, the wavefunctions of different scatterers will not overlap to a significant degree, and the symmetry of the wavefunction need not be considered.

For exchange of momentum Δp_μ at the j^{th} site, $\overline{\psi}_s$ in (2) must be replaced by

$$\overline{\psi}_s' = \psi_{soj}^{*} a_{oj}^{\dagger} e^{-\frac{i \Delta p_\mu x^\mu}{\hbar}} + \sum_{i \neq j} \psi_{soi}^{*} a_{oi}^{\dagger} \qquad (8)$$

We may write (8) in a more illuminating form by adding $\psi_{soj}^{*} a_{oj}^{\dagger}$ to the last term and subtracting it from the first term to give

$$\overline{\psi}_s' = \psi_{soj}^{*} a_{oj}^{\dagger} \left[e^{-\frac{i \Delta p_\mu x^\mu}{\hbar}} - 1 \right] + \sum_{ALL\ N} \psi_{soi}^{*} a_{oi}^{\dagger} \qquad (8A)$$

In (8A) the last term gives the probability amplitude for the possible process where no momentum is exchanged at any site. The first term then gives the contribution to the amplitude for exchange Δp_μ at the j^{th} site. Since we are assuming strong coupling of nuclei to each other with no possibility of identifying the scattering site, we must sum only the first term in (8A) over all possible sites, when computing the S matrix (1).

This gives, for coherent momentum transfer phase shift scattering

$$S = \frac{\bar{U}_{If} K U_{Io}}{\hbar c V} \int \sum_{n=1}^{n=N} \left(\frac{\alpha}{\pi}\right)^{3/2} e^{-\alpha|\bar{r}-\bar{r}_n|^2 + \frac{i}{\hbar}(p_{Io}-p_{If}-\Delta p)_\mu x^\mu} d^4x \qquad (9)$$

SCATTERING CROSS SECTIONS

Suppose now that we have nuclei in a cubic crystal with N identical cells each with length a. For these assumptions the S matrix (9) for initial and final states in which the harmonic oscillator quantum numbers are the same, is given by

$$S = \bar{U}_{If} K U_{Io} X Y Z T \left(\frac{1}{\hbar V}\right) \qquad (10)$$

with

$$X = \sum_{n=1}^{n=N^{1/3}} e^{\frac{i}{\hbar}(p_{Io}-p_{If}-\Delta p)_x x_n - \frac{1}{\alpha}\left(\frac{p_{Io}-p_{If}-\Delta p}{2\hbar}\right)_x^2}$$

In (10), $x_n = n a$, with corresponding definitions for Y and Z. As before, α is a parameter specifying the width of the harmonic oscillator wavefunction.

$$T = \frac{\sin\left[\frac{(E_{If}-E_{Io}+E_{Sf}-E_{So})\tau}{2\hbar}\right]}{\left[\frac{E_{If}-E_{Io}+E_{Sf}-E_{So}}{2\hbar}\right]} \qquad (11)$$

E_{If} and E_{Sf} are the final state energies of the incident particle and ensemble of scatterers respectively, E_{Io} and E_{So} are the corresponding original energies.

The scattering cross section is given by σ, with

$$\sigma = \sum \frac{V(S-1)^2}{c\tau} = \frac{V}{(2\pi)^6 c\tau\hbar^8} \int \left| \bar{U}_{IF} K U_{IO} X Y Z T \right|^2 d\bar{p}_S\, d\bar{p}_I \qquad (12)$$

In (12) $d\bar{p}_S$ is the element of momentum space for the final state of the ensemble of scatterers, $d\bar{p}_I$ is the element of momentum space for the final state of the incident particle. T in (11) and (12) is a function of the momentum variables in X, Y, and Z. The integration (12) is carried out in the following way:

The length L of the crystal is given by $L = aN^{1/3}$, to a very good approximation we may evaluate

$$\frac{L}{2\pi\hbar}\int X^2 dp_{Sx} = \frac{L}{2\pi\hbar}\int \left[\frac{\sin\left(\frac{N^{1/3}a\,[p_{IO}-p_{IF}-\Delta p]_x}{2\hbar}\right)}{\sin\left(\frac{a\,[p_{IO}-p_{IF}-\Delta p]_x}{2\hbar}\right)}\right]^2 e^{-\frac{\varepsilon}{\alpha}\left(\frac{p_{IO}-p_{IF}-\Delta p}{2\hbar}\right)^2} dp_{Sx} = N^{2/3} \qquad (13)$$

Combining (13), (12) and (11) then gives

$$\sigma = \frac{N^2\left(\bar{U}_{IF} K U_{IO}\right)^2}{(2\pi)^3 c\hbar^5\tau}\int T^2 d\bar{p}_I = \frac{N^2\left(\bar{U}_{IF} K U_{IO}\right)^2}{(2\pi)^3 c\hbar^5\tau}\int (T p_I)^2 \frac{d|p_I|}{dE}\, dE\, d\Omega_I \qquad (14)$$

with $E = E_I + E_S$, $d\Omega_I$ is the element of solid angle into which the incident particle is scattered.

In the center of mass system

$$\frac{d|p_I|}{dE} = \frac{E_{IF}E_{SF}}{c^2 p_I (E_{IF} + E_{SF})} \qquad (15)$$

(14) is integrated over E first

$$\sigma = \frac{N^2 (\bar{v}_{If} K U_{Io})^2}{4\pi^2 c^3 \hbar^4} \int P_I \frac{E_{If} E_{sf}}{(E_{If} + E_{sf})} d\Omega_I \qquad (16)$$

(13) implies that

$$d\Omega_I \sim \left[\Delta p + \frac{2\hbar\pi}{N^{1/3} a}\right]^2 \frac{1}{(P_{Io})^2}$$

The integral (16) is over all values of Ω which approximately conserve energy and momentum as implied by the integrations (13) and (14). It can be shown for the case of zero rest mass particles, that a large volume of phase space meets these criteria. (16) may approach N^2 times the cross section of a single particle on one site.

The result (16) was obtained for the very simple cubic model. A similar result may be obtained for any very tightly bound group of scatterers even if these are not arranged in a perfect periodic lattice. For the more general case we may define

$$f(\bar{p}_{If} - \bar{p}_{Io} - \Delta\bar{p}) = \int e^{\frac{i}{\hbar}(\bar{p}_{If} - \bar{p}_{Io} - \Delta\bar{p})\cdot r'} \psi^*_{so}(r') \psi_{so}(r') d\bar{r}' \qquad (17)$$

$$R = f(\bar{p}_{If} - \bar{p}_{Io} - \Delta\bar{p}) \sum_{n=1}^{n=N} e^{\frac{i}{\hbar}(\bar{p}_{If} - \bar{p}_{Io} - \Delta\bar{p})\cdot \bar{r}_n} \qquad (18)$$

In terms of (17) and (18) the S matrix is

$$S = \frac{\bar{v}_{If} K U_{Io} R T}{\hbar V} \qquad (19)$$

R may be evaluated in the following way. In (18) consider the sum

$$\sum_{n=1}^{n=N} e^{\frac{i}{\hbar}(\bar{p}_{IF}-\bar{p}_{IO}-\Delta\bar{p})\cdot\bar{r}_n} \tag{20}$$

and express it as the product of factors involving X_n, Y_n, Z_n

$$\sum_{n=1}^{n=N_x} e^{\frac{i}{\hbar}(\bar{p}_{IF}-\bar{p}_{IO}-\Delta\bar{p})X_n} \sum_{n=1}^{n=N_y} e^{\frac{i}{\hbar}(p_{IF}-p_{IO}-\Delta p)_y Y_n} \sum_{n=1}^{n=N_z} e^{\frac{i}{\hbar}(p_{IF}-p_{IO}-\Delta p)_z Z_n} \tag{21}$$

the object

$$X' = \sum_{n=1}^{n=N_x} e^{\frac{i}{\hbar}(p_{IF}-p_{IO}-\Delta p)_x X_n} \tag{22}$$

is the sum of N_x unit vectors. The last one in the sum makes an angle

$$\theta_{N_x} = \frac{i}{\hbar}(p_{IF}-p_{IO}-\Delta p)_x X_N \tag{23}$$

with the first. The increments in angle are not equal, however the sum is given approximately by

$$X' = N_x \frac{\sin\frac{\theta_{Nx}}{2}}{\frac{\theta_{Nx}}{2}} \tag{24}$$

Similar expressions result for Y' and Z', and

$$R = X'Y'Z' f(p_{IF}-p_{IO}-\Delta p) \tag{25}$$

The phase space integrals then give a result similar to (16).

DISCUSSION

The large cross sections (16) result from three very important assumptions. The ensemble of scatterers is assumed to be infinitely stiff, and recoils in the same manner as a single elementary particle on the N sites. Expression (8) then states that a final ensemble state differs from an initial state only in the phase factor $e^{\frac{i\Delta p_r x^r}{\hbar}}$. This phase factor is crucial for obtaining a large cross section because it may enormously increase the solid angle into which scattering occurs.

Suppose first that the phase factor $e^{\frac{i\Delta p_r x^r}{\hbar}}$ is absent -- as in the published solutions for potential scattering -- in which energy but not momentum is conserved.[4] The absence of Δp_r may enormously decrease the value of (16), because under this condition the expressions for X^2, Y^2, Z^2, and (13) imply

$$\frac{N^{1/3}a\,(p_{Io}-p_{If})}{2\hbar} << \pi \qquad (26)$$

(26) then limits the solid angle into which scattering may occur, expression (16), to

$$\Delta\Omega < \left(\frac{2\hbar\pi}{N^{1/3}a}\right)\frac{1}{p_{Io}^2} = \left[\frac{2\pi(\text{DE BROGLIE WAVELENGTH OF INCIDENT PARTICLE})}{\text{LENGTH OF SCATTERER ARRAY}}\right]^2 \qquad (27)$$

The limitation of the Ω integration by (27) results in an extremely small cross section. This limit disappears when the phase factor $C^{\frac{i\Delta p_r x''}{\hbar}}$ is included, for Δp_r the same value for all scatterers.

This follows from the modification of (27) as a result of the collective momentum transfer phase shift, to

$$\Delta\Omega < \left[\Delta p + \frac{2\hbar\pi}{N^{1/3}a}\right]^2 \frac{1}{(p_{I0})^2} \qquad (28)$$

For large N, if $\Delta p \to p_{I0}$, (28) is enormously greater than (27). The cross section (16) and transition probabilities are correspondingly increased.

The second assumption is that the ensemble consists of highly localized particles which do not, therefore, have well defined momenta. It can be shown that if the momenta of all scatterers are precisely known before and after the interaction with the incident beam, the total cross section (and transition probability) will be very small.

The third assumption is that the sign of the interaction is the same in all volume elements. For electromagnetic radiation incident on a solid this requires an applied nearly uniform field to obtain essentially the same polarization in all volume elements. For the neutrino field, the universal Fermi interaction has the same sign for all relevant elements of volume.

MOMENTUM TRANSFER CONSIDERATIONS

If the scatterers are not tightly bound, exchange of momentum at only one site permits identification of that site. Coherence is lost for the single particle momentum exchange process. However such an ensemble may exchange Δp with N scatterers, each one contributing $\frac{\Delta p}{\sqrt{N}}$ on average. For large N the total cross section is small because the solid angle is limited as implied by (27).

For the tightly bound case we may imagine processes in which 2,3, ... up to N scatterers exchange total momentum Δp. It can be shown that the single unidentified scatterer case gives the largest cross section.

INTERACTION OF LOW ENERGY ANTINEUTRINOS WITH A CRYSTAL

The operators of expression (1) are chosen to be those of the neutral current antineutrino interactions with scatterers which may have spin. The elastic scattering cross section, following (1) through (12) is given by

$$\sigma = \frac{G_w^2 N^2}{4\pi^2 \hbar^4 c^4} \int E_\nu^2 \langle (\bar{U}_{s0} \gamma^\alpha (1+\gamma_5) U_{\nu 0} \bar{U}_{\nu f} \gamma_\alpha (1+\gamma_5) U_{s0})^2 \rangle d\Omega_\nu \qquad (12A)$$

In (12A), E_ν is the antineutrino energy, G_w is the weak interaction coupling constant, $\bar{U}_{s0}$ is the creation operator for a scatterer, γ^α are the matrices of the Dirac equation, $\gamma^5 = -i\gamma^0\gamma^1\gamma^2\gamma^3$, $\bar{U}_{\nu f}$ is a creation operator for the final state of the antineutrino, $U_{\nu 0}$ is an annihilation operator for the initial state of the antineutrino. $d\Omega_\nu$ is the solid angle into which the antineutrino is scattered. For unpolarized scatterers (12A) is the same for neutrinos and antineutrinos and is evaluated to be

$$\sigma = \frac{4 G_w^2 E_\nu^2 N^2}{\pi \hbar^4 c^4} \qquad (12B)$$

An ongoing experiment employs antineutrinos from a tritium source. The target is a single crystal of sapphire 2.5 cms. in diameter and 0.38 cms. in thickness. A total cross section approximately two cms^2. is observed, in reasonable agreement with the theory presented here.

INTERACTION OF PHOTONS WITH AN ENSEMBLE OF NUCLEAR MOMENTS

To study the interaction of light with nuclear moments, a crystal is selected which is transparent in the absence of applied magnetic fields. A moderate magnetic field is employed to polarize the nuclei. Each nucleus is assumed to have magnetic moment μ given by

$$\mu = g\mu_0 \, I \tag{29}$$

In (29) g is the gyromagnetic ratio, I is the spin vector in units of $\hbar$, μ_0 is the nuclear magneton given in terms of the nuclear mass M, electron charge e, and speed of light c, by

$$\mu_0 = \frac{e\hbar}{2M_n c} \tag{30}$$

The Maxwell vector potential operator is given, in Coulomb gauge by

$$A_i = \sqrt{\frac{2\pi\hbar c}{V}} \sum_k \frac{1}{\sqrt{2k}} \sum_{m=1}^{m=3} \left(a_m(k)\epsilon_i^m e^{ik_\mu x^\mu} + a_m^\dagger(k)\epsilon_i^m e^{-ik_\mu x^\mu} \right) \tag{31}$$

In (32), $a_m^\dagger(k)$ and $a_m(k)$ are creation and annihilation operators, respectively, for photons. ϵ_i^m are a pair of orthonormal unit vectors, in a plane perpendicular to $\bar{k}$

For interaction of electromagnetic radiation with nuclear moments, the S matrix is given by

$$S = \frac{g\mu_0}{\hbar c} \int \langle F | \psi_s^\dagger \psi_s \epsilon^{abc} I_a \frac{\partial A_b}{\partial x^c} | 0 \rangle \, d^4x \tag{32}$$

In (32) ϵ^{abc} is the three space Levi Civita tensor density. It is zero if two indices are equal and unity if all indices are different. $\epsilon^{123} = +1$ and changes sign on the interchange of any pair of indices.

For N scatterers in harmonic oscillator ground states, (32) is evaluated as

$$S = g\mu_0 \sqrt{\frac{4\pi k}{cV\hbar}} \int \sum_{n=1}^{n=N} \left(\frac{\alpha}{\pi}\right)^{3/2} e^{-\alpha|\bar{n}-\bar{n}_n|^2 + \frac{i}{\hbar}(p_0 - \Delta p)\cdot x^\nu} \langle F|\eta\cdot I|0\rangle \, d^4x \tag{33}$$

In (33) $\bar{\eta}$ is an appropriate unit vector defined by (32), in the direction of the incident light magnetic field. (33) may be written in terms of the integrals X, Y, Z, T defined earlier with (10), as

$$S = g\mu_0 \sqrt{\frac{4\pi ck}{V\hbar}} \, XYZT \langle F|\eta\cdot I|0\rangle \tag{34}$$

Following the procedures of (12), (13) and (14), the cross section for absorption, or emission, is computed to be

$$\sigma = (2\pi)^7 \mu_0^2 k g^2 \hbar^{-4} N_\mu^2 \tau^{-1} |\langle F|\eta\cdot I|0\rangle|^2 L^3 \int X^2 Y^2 Z^2 T^2 \rho(E) dE \, d\bar{p}_s \tag{35}$$

$$= 8\pi^2 k \mu_0^2 g^2 \rho(E) |\langle F|\eta\cdot I|0\rangle|^2 N^2$$

N is the total number of spins. All are regarded as being in the same quantum state. The difference between the number parallel and antiparallel is contained within the squared matrix element.

Expression (35) will usually greatly exceed the area of the crystal implying total extinction in passage of light through the first portion of the crystal traversed by the light.

A real crystal is much more than an ensemble of nuclear spins. Each nuclear spin is enclosed by electron shells. The electrons contribute dynamic diamagnetism which may greatly change the light intensity at the nuclei from the free space value. Therefore (35) will not generally give quantitatively accurate results without the electron shell corrections.

COHERENT ABSORPTION OR SIMULATED EMISSION ISSUES

The theory given earlier in equations (10)-(14) considered an incident particle with momentum P_{IO} scattered into momentum P_{IF} with momentum exchange $\Delta\bar{P}$. For the experiments reported here the incident particle may be absorbed and P_{IF} is zero, or there may be stimulated emission. Here again the single scatterer exchange $\Delta\bar{P}$ is required to give a large cross section. Without the exchange $\Delta\bar{P}$, the total cross section will in general be much smaller than (35), because the denominators of X,Y,Z, will not approach zero.

Conservation of Momentum and Energy

For the process being considered, a photon is absorbed or created by the ensemble of scatterer magnetic moments. The entire ensemble recoils and its change of momentum Δp is balanced by the gain or loss of the photon momentum. Since the mass of the magnetic moments is very large, the recoil energy will be very much smaller than the photon energy,

$$E_{RECOIL} << c\Delta p \tag{36}$$

Energy may be conserved if the spin system state is changed. The interaction will not be coherent over all N particles if the interaction changes the spin states of certain ones because these could then be identified as causing the interaction .

Here it is assumed that all interacting particles are in the same kind of quantum state and all are changed in the same way by the interaction. Suppose the magnetic moments are associated with spin ½ particles. Every particle is assumed to have the spin state $\psi_0 = \begin{vmatrix} a_{1S} \\ a_{2S} \end{vmatrix}$ which is changed by the interaction to $\psi_F = \begin{vmatrix} a'_S \\ a'_S \end{vmatrix}$ To conserve energy it is necessary that

$$N\left[|a_S|^2 - |a_S|^2 - |a'_S|^2 + |a'_S|^2\right]\mu H_0 = \hbar\omega \tag{37}$$

A study of the integrations (33), (34), and (35) indicates that energy exchange as implied by (37) may occur in more than one way, without significant reduction of the total cross section. Each site interacts with the incident light, and a process in which momentum is exchanged at one site, and energy exchanged at many other sites simultaneously, leads to the large value (35). It can also be imagined that both energy and momentum are exchanged at a single site, and other interactions distribute the energy to the ensemble of nuclear spins.

Net Exchange of Energy

In spectroscopy and quantum electronics the interaction of radiation with a large number of particles in thermal equilibrium is usually described by the density matrix with random phases. For a particle with two quantum states U_1 and U_2, with energies E_1 and E_2, an equivalent description is to assume that N_1 are in the state U_1, N_2 are in the state U_2, and

$$N_2 = N_1 e^{-(E_2-E_1)/kT} \tag{38}$$

If spontaneous emission is not important and the transition probability for stimulated emission is W_{12}, the net power exchanged is P_{net}, given by

$$P_{NET} = W_{12}(N_1 - N_2)\hbar\omega_{12} \tag{39}$$

For the coherent process being considered here all particles are assumed to be in the same spin state. For spin ½ the wavefunction for each particle is

$$\psi = a_{1S}U_1 + a_{2S}U_2 \tag{40}$$

The instantaneous net power exchanged is P^I_{net}

$$P^I_{NET} = N\frac{d}{dt}\left[|a_{1S}|^2E_1 + |a_{2S}|^2E_2\right] \tag{41}$$

Unitarity requires

$$|a_{1S}|^2 + |a_{2S}|^2 = 1 \tag{42}$$

(41) and (42) give

$$P^{I}_{NET} = N(E_1 - E_2)\frac{d}{dt}|a|^2 \tag{43}$$

(42) and (43) then give

$$P^{I}_{NET} = \frac{N}{2}(E_1 - E_2)\frac{d}{dt}\left(|a_{1S}|^2 - |a_{2S}|^2\right) \tag{44}$$

If the system remains in thermal equilibrium

$$|a_{2S}|^2 = |a_{1S}|^2 e^{-\frac{E_{21}}{kT}} \tag{45}$$

the average net power is then

$$\langle P_{NET} \rangle = \frac{N}{2}(E_1 - E_2)\frac{d}{dt}\left[|a_{1S}|^2\left(1 - e^{-\frac{E_{21}}{kT}}\right)\right] \tag{46}$$

Density of States and Matrix Elements

For the reported experiments, crystals of Lithium Flouride and Sapphire interact with light from Helium Neon Lasers. The transmitted light is measured with a photometer outside of the magnetic field. Changes are observed as the magnetic field is varied. (Figure 1) We may expect the density of states $\rho(E)$ in (35) to be given by

$$\rho(E) = \frac{1}{\hbar\omega_{NMF}} \tag{47}$$

Making use of (47) enables us to write the total cross section (35) in terms of the fine structure constant α_f, the Compton wavelength λ_{CN} of the scatterers, the angular frequency ω_L of the incident light, and the nuclear magnetic resonance angular frequency ω_{NMR} in the applied time independent magnetic field H_0 as

$$\sigma = 2\pi^2 \alpha_f \left(\frac{\omega_L}{\omega_{NMR}}\right) \lambda_{CN}^2 \left|\langle F|\eta\cdot I|0\rangle\right|^2 N_\mu^2 g^2 \qquad (35\Lambda)$$

In order to complete the calculation for the expected coherent absorption of light by an ensemble of magnetic moments we must evaluate the squared matrix element

$$\left|\langle F|\eta\cdot I|0\rangle\right|^2 \qquad (48)$$

(48) is the square of the matrix element of the component of spin parallel to the magnetic field of the incident light.

EFFECTS OF AN APPLIED RADIOFREQUENCY FIELD AT THE NUCLEAR MAGNETIC RESONANCE FREQUENCY

Consider an isolated particle with spin $\frac{1}{2}$ having the wavefunction (40). Application of a radiofrequency magnetic field normal to the constant magnetic field at the exact resonance frequency will modify (40). Integration of the Schroedinger equation for interaction of a magnetic moment with the fields gives

$$\psi = \begin{vmatrix} e^{-\frac{i\omega_{NMR}t}{2}}\left[a_{1S}\cos\frac{\omega_1 t}{2} - i a_{2S}\sin\frac{\omega_1 t}{2}\right] \\ e^{\frac{i\omega_{NMR}t}{2}}\left[-i a_{1S}\sin\frac{\omega_1 t}{2} + a_{2S}\cos\frac{\omega_1 t}{2}\right] \end{vmatrix} \qquad (40A)$$

In (40A), ω_1 is given by

$$\omega_1 = \frac{\omega_{NMR}\, H_{RADIOFREQUENCY\ NMR}}{H_0} \qquad (40B)$$

The expectation values of the x, y, and z components of the nuclear spin are calculated from (40A) to be

$$\langle \sigma_z \rangle = \left\langle |a_{1S}|^2 - |a_{2S}|^2 \right\rangle \cos\omega_1 t + i\langle a_{2S}^* a_{1S} - a_{1S}^* a_{2S}\rangle \sin\omega_1 t \qquad (49)$$

$$\langle \sigma_x \rangle = \left\langle \left(|a_{1S}|^2 - |a_{2S}|^2\right)\sin\omega_{NMR}t \sin\omega_1 t + i\langle a_{1S}^* a_{2S} - a_{1S} a_{2S}^*\rangle \sin\omega_{NMR}t\cos\omega_1 t \right. \qquad (50)$$
$$\left. + \langle a_{1S}^* a_{2S} + a_{1S} a_{2S}^*\rangle \cos\omega_{NMR}t \right\rangle$$

$$\langle \sigma_y \rangle = \langle |a_{2S}|^2 - |a_{1S}|^2\rangle \cos\omega_{NMR}t \sin\omega_1 t + i\langle a_{1S} a_{2S}^* - a_{1S}^* a_{2S}\rangle \cos\omega_{NMR}t\cos\omega_1 t \qquad (51)$$
$$+ \langle a_{1S}^* a_{2S} + a_{1S} a_{2S}^*\rangle \sin\omega_{NMR}t$$

ω_{NMR} is very large, ω_1 is very small. Since the incident light magnetic field is parallel to the time independent magnetic field, $\langle \sigma_z \rangle$ is believed to dominate the optics experiments discussed here in accordance with (48). $\langle \sigma_x \rangle$ and $\langle \sigma_y \rangle$ are usually observed in nuclear magnetic resonance.

EXPERIMENTS

Red light of wavelength 632.8 nm from a one milliwatt Helium Neon Laser was employed with the apparatus of Figure 1. Interaction of a small part of this light with lithium fluoride, and sapphire crystals was observed as a function of applied magnetic field at 4.2 Kelvin. A silicon solar cell A served as a photometer.

A photometer may have its calibration affected by magnetic fields as a result of the interaction of photoelectrons with such fields. To reduce this effect, a magnetic shield was constructed from an iron alloy as indicated in Figure 1. The crystal was removed and the Laser light directly transmitted to the photometer. Experiments indicated that for light intensities and magnetic fields of the present experiments, the magnetic shield was effective. It maintained the calibration of the photometer to better than five percent as the magnetic field was varied from zero to its maximum value of 8000 Gauss.

For large N (37) requires the final spin state $\begin{vmatrix} a'_{1S} \\ a'_{2S} \end{vmatrix}$ to be very nearly the same as the initial spin state $\begin{vmatrix} a_{1S} \\ a_{2S} \end{vmatrix}$. For this case the squared matrix element (48) will differ from zero only if the vector $\vec{n}$ has a component parallel to the applied magnetic field. An "unpolarized" Laser was employed for the initial experiments. Its output was found to be polarized. The laser was rotated so that the magnetic field vector of its light output was parallel to the applied magnetic field, at the beginning of the experiment.

The Laser had outputs at 632.8 nm and at 3300 nm. Neutral density filters and an infra red filter were employed. These reduced the infra red output to less than 10^{-14} watts. Approximately 10^{-12} watts of 632.8 nm light reached the photometer with zero applied magnetic field. A lens diffused the light so that the entire crystal cross section was illuminated.

A magnetic field of strength approximately 8000 Gauss was applied, with crystal and photometer at 4.2 Kelvin. This reduced the intensity of the light measured by the photometer by a factor about 2.* Then on a time scale of hours,

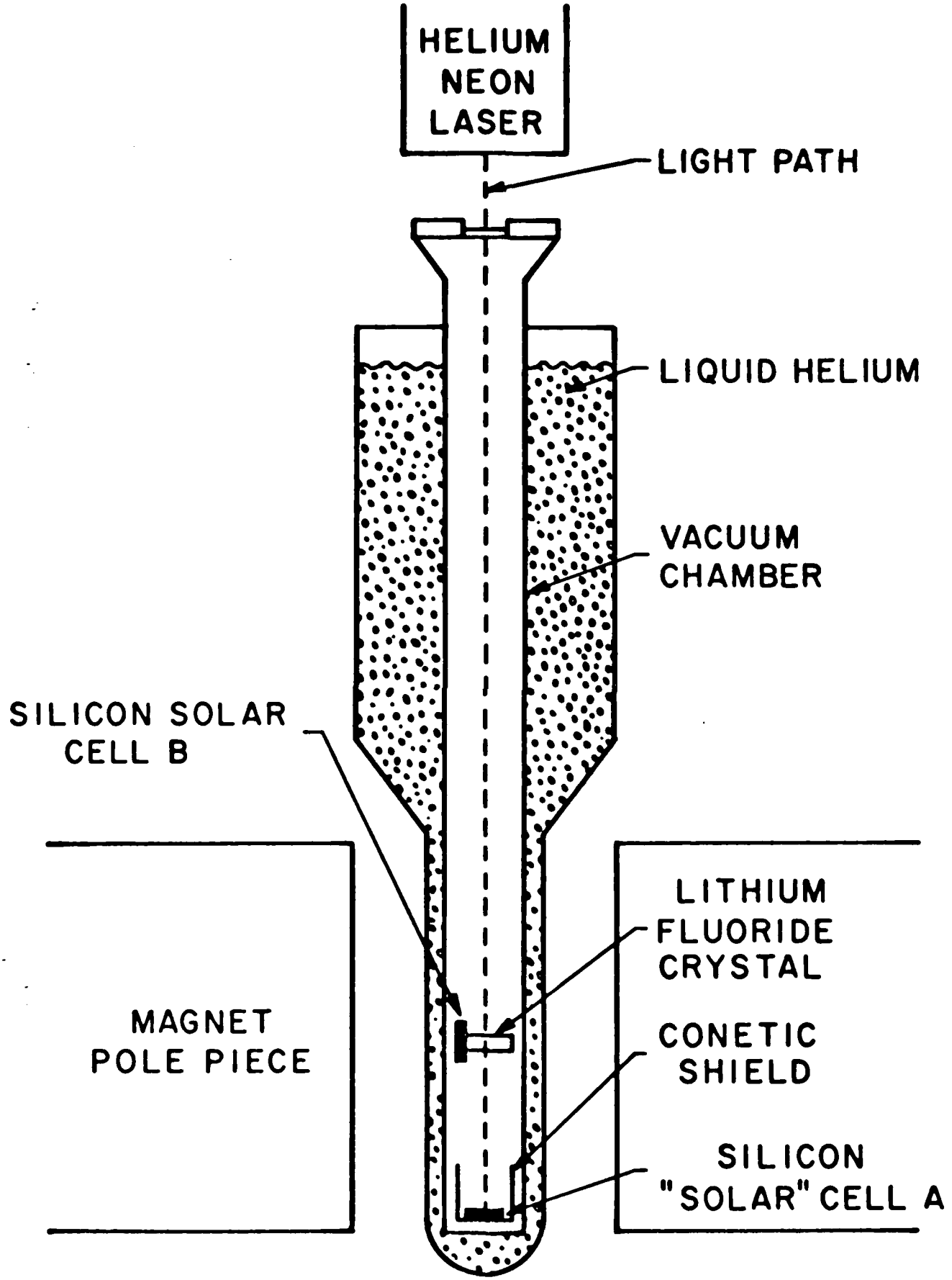
HELIUM
NEON
LASER
LIGHT PATH
LIQUID HELIUM
VACUUM
CHAMBER
SILICON SOLAR
CELL B
MAGNET
POLE PIECE
LITHIUM
FLUORIDE
CRYSTAL
CONETIC
SHIELD
SILICON
"SOLAR" CELL A

FIGURE 1

* The very short relaxation time phenomena associated with magnetic field changes may be due to paramagnetic impurities. If these are present in a concentration of one part in 10^7 their collective interaction with light may produce large changes. In expressions (35) and (35A) the cross section is proportional to the product of the square of the magnetic moment and the square of the difference in moments parallel and antiparallel to the field. Both of these factors are very much greater for electrons than for nuclei, and compensate for the small paramagnetic concentration. Estimates for the case of very small coupling between these magnetic moments give results in reasonable agreement with observations.

the intensity changed, undergoing oscillations as shown in Figure 2. Eventually, in some cases after more than 20 hours, the intensity dropped to a value less than ten percent of the photometer output with no applied magnetic field.

FIGURE 2

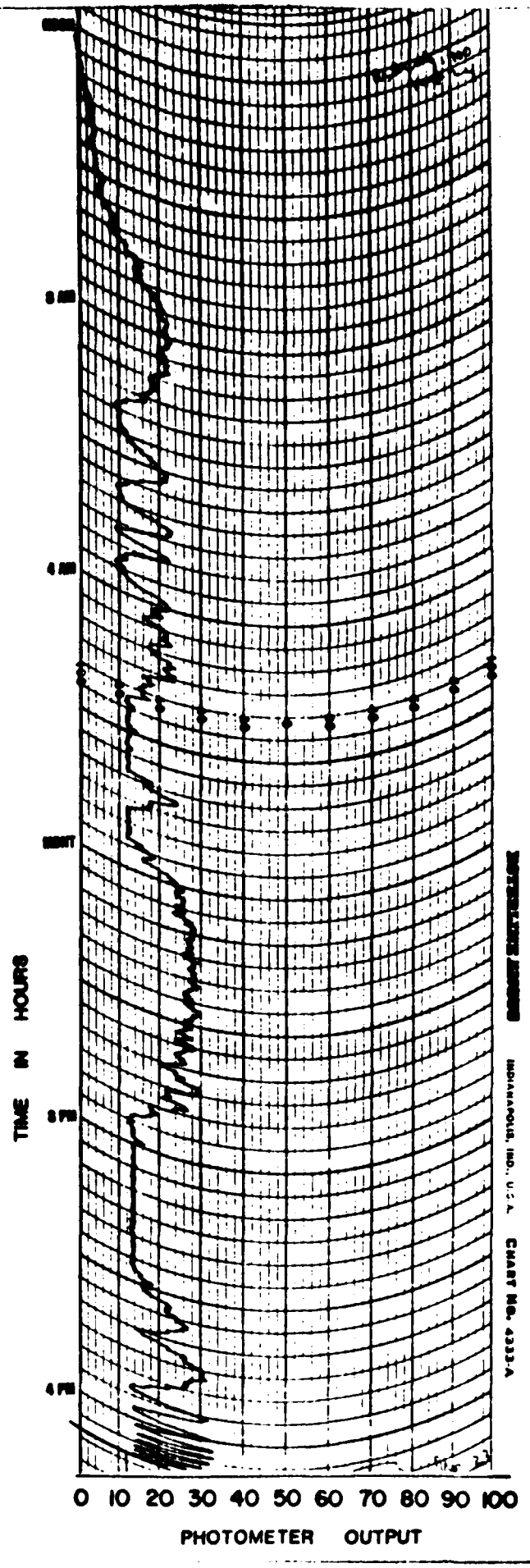
TIME IN HOURS
0 10 20 30 40 50 60 70 80 90 100
PHOTOMETER OUTPUT
INDIANAPOLIS, IND., U.S.A.
CHART NO. 4333-A

Refilling was required at least once in 24 hours. The enormous vibration levels which accompany transfer of liquid helium result in phonon densities sufficiently great to again excite the kind of oscillations shown in Figure 2.

Removal of the magnetic field again resulted in a long period relaxation, exceeding 6 hours, shown in Figure 3, back to the small attenuation levels.

Similar results were obtained with a sapphire crystal as shown in Figure 4.

With no applied radiofrequency fields, no evidence for a resonance in absorption of light was found as a function of the applied magnetic field.

The process described by (32) is an absorption of photons. The observed decrease in intensity might also be understood in terms of a higher order elastic scattering process. To check this possibilit a second photometer B was employed as shown in Figure 1. The crystal was cut and polished along a plane parallel to its axis and the polished face was covered by a silicon "solar" cell. The second photometer then observes light scattered at right angles to the incident rays. If the observed decrease in the direct light to photometer A is the single photon coherent absorption of equation (35), the outputs A and B should both decrease. If the observed decrease of

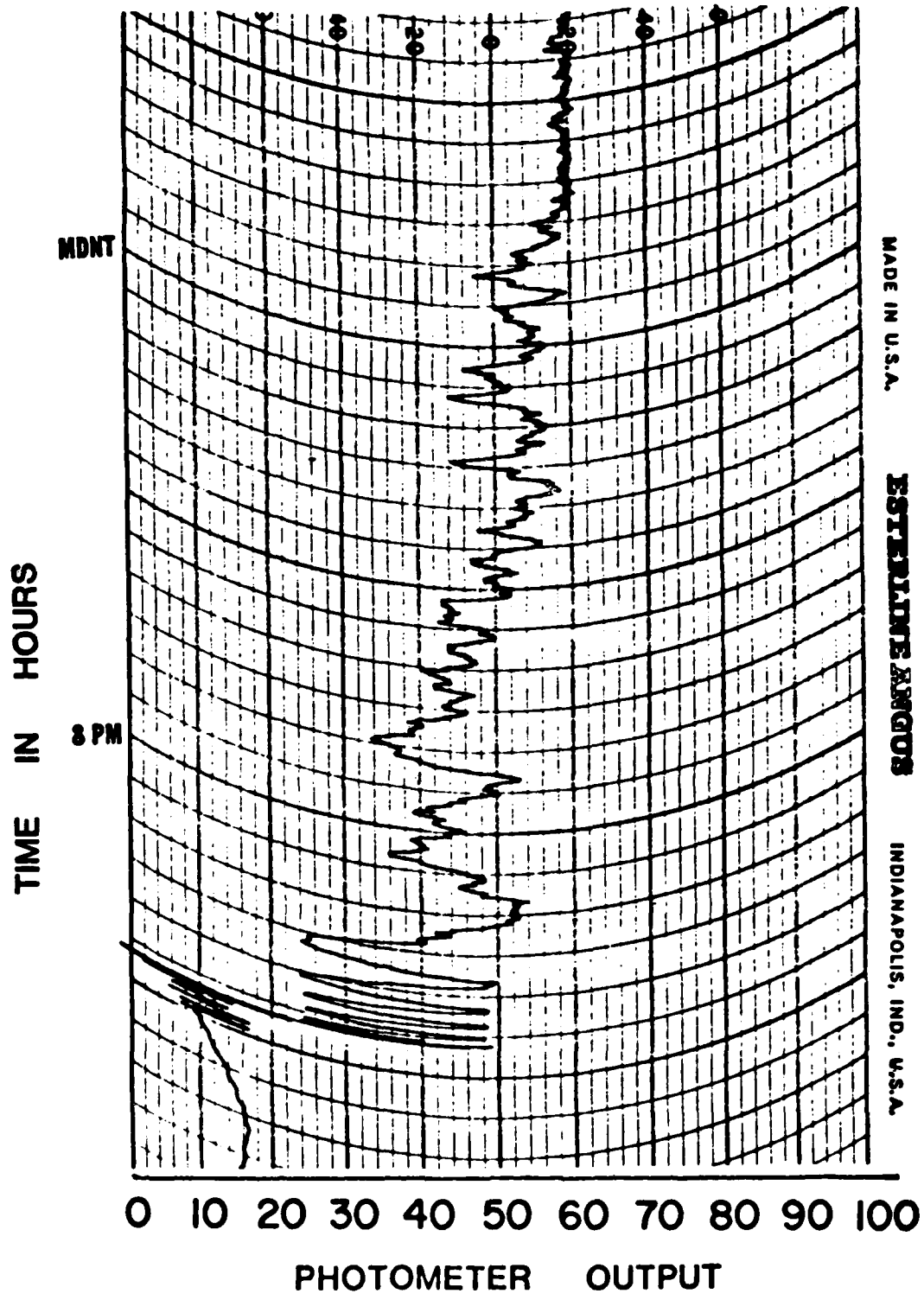
MDNT
8 PM
TIME IN HOURS
MADE IN U.S.A.
ESTERLINE ANGUS
INDIANAPOLIS, IND., U.S.A.
0 10 20 30 40 50 60 70 80 90 100
PHOTOMETER OUTPUT

FIGURE 3

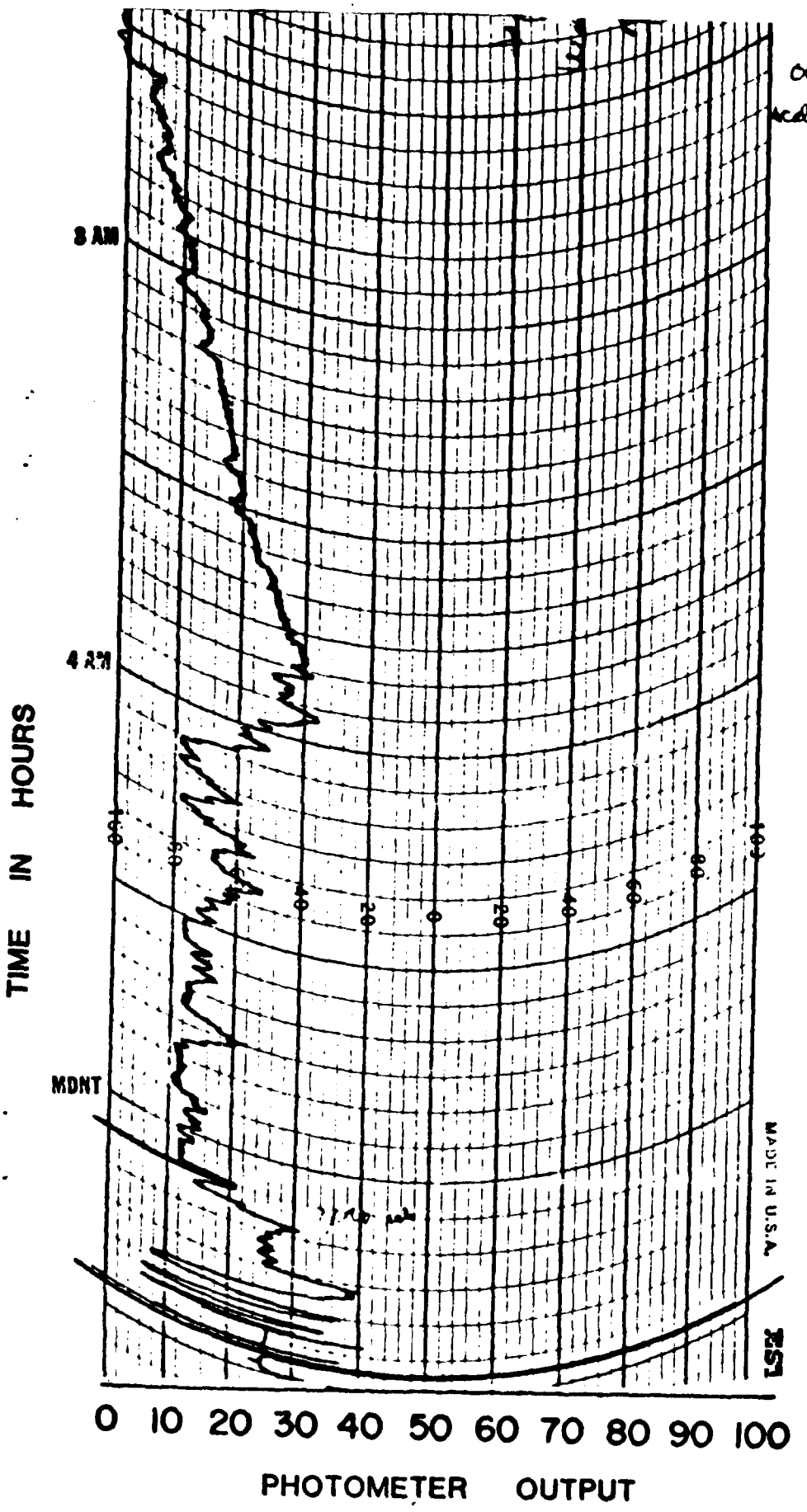
8 AM
4 AM
MDNT
TIME IN HOURS
0 10 20 30 40 50 60 70 80 90 100
PHOTOMETER OUTPUT

FIGURE 4

intensity in A is associated with elastic scattering, a decrease in A should be accompanied by an increase in B. All observations gave decreases in B when the direct light to A was observed to decrease. With reduction of the applied magnetic field, both photometer outputs increased. Within limits of experimental error the two photometer outputs always changed in the same direction by approximately the same fractional amounts.

Possible Heating Effects

A spin 1/2 system has specific heat C_v given by

$$C_v = \frac{\partial}{\partial T} \frac{N\epsilon}{\left(e^{\epsilon/kT} + 1\right)} \approx \frac{Nk}{4}\left(\frac{\epsilon}{kT}\right)^2 \approx 10^{-7}$$ Joules per degree

at 4K for the Fluorine nuclei in the crystal for an 8,000 Gauss field.

At the intensity 10^{-12} watts, more than one day would be required to significantly heat the spin system. To check this conclusion the light source was turned off for an hour, after the system appeared to be in equilibrium. Restoring the light intensity to the earlier value reproduced the earlier result.

Two lithium fluoride crystals were employed, both furnished by Harshaw. Both had been irradiated by x rays to permit easier grinding and polishing. One had been annealed. It was colorless.

A nuclear magnetic resonance spectrometer was developed as shown in Figure 6. The spin lattice relaxation time for the Fluorine atoms was measured and found to be approximately three hours. The crystal which had not been annealed, appeared to be very light yellow, and measurements gave a spin lattice relaxation time approximately 40 minutes. Allowing for the difference in relaxation times, both crystals responded to light and radiofrequency fields in the same way.

To further explore the issue of correlations, the radiofrequency field was modulated at one hertz. The light output was amplified by a synchronous detector switched at the one hertz modulation frequency. Figure 5 shows the correlations. The upper trace is the recorded nuclear magnetic resonance output as the applied magnetic field was slowly swept through resonance. The lower trace is the light output from the synchronous detector at the same time. Figure 7 is for the same kind of data with signal averaging over six complete cycles to improve the signal to noise ratio. A radiofrequency field considerably less than required for saturation was employed. The observed correlations for this relatively small radiofrequency field are roughly one percent of the light output.

At other times the magnitude of the correlations varied considerably, depending on the spin state history.

It was then decided to search for correlations in the output of the nuclear magnetic resonance spectrometer with the incident light. Such correlations were found to be large at certain values of incident light intensity. At a power $\sim 10^{-9}$ watts from the helium neon laser, opening and closing the shutter produced the large changes in radiofrequency output shown in Figure 8, for the spectrometer tuned exactly to the Fluorine resonance. The spin state history

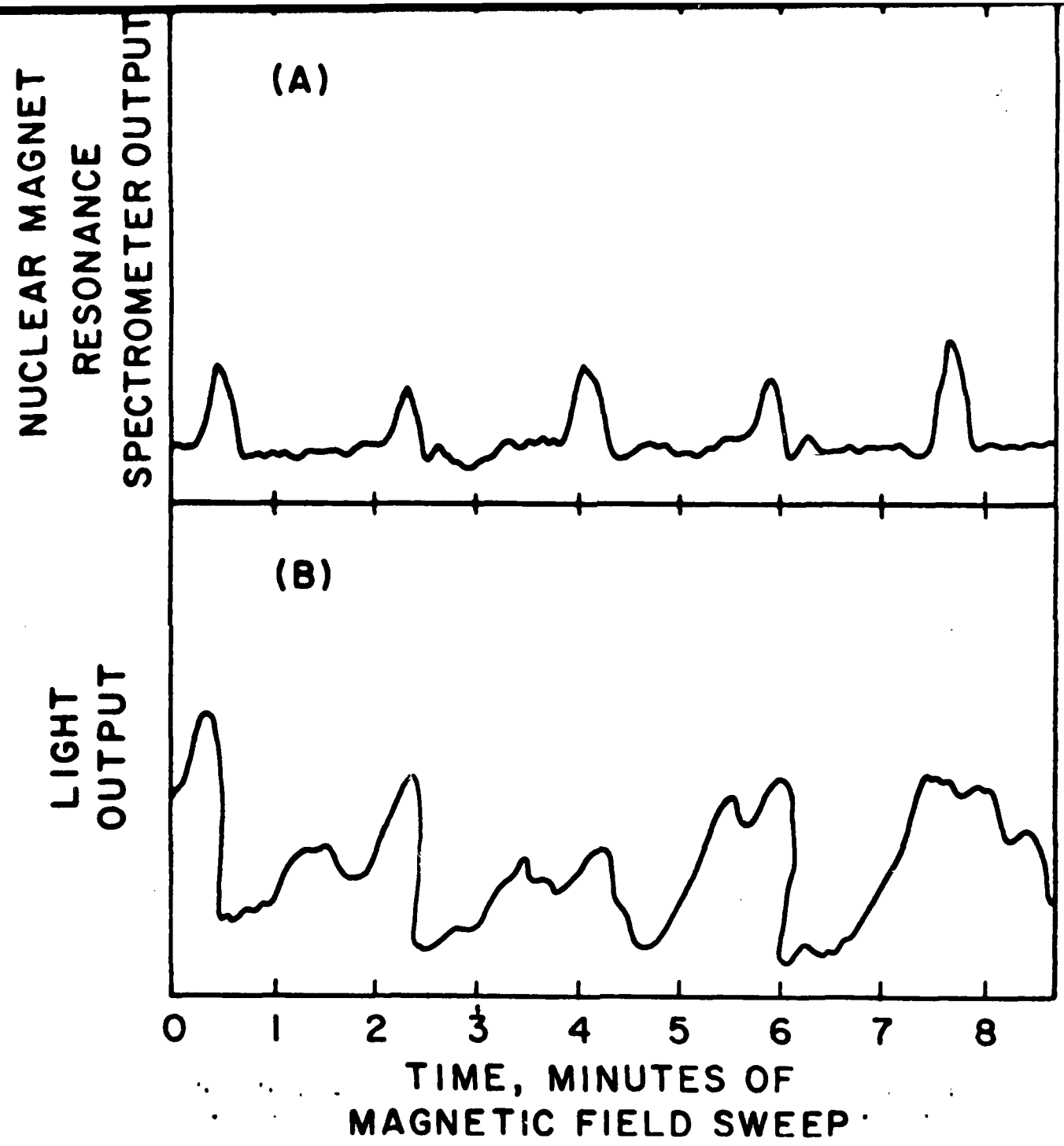
(A)
NUCLEAR MAGNET RESONANCE SPECTROMETER OUTPUT
(B)
LIGHT OUTPUT
0
1
2
3
4
5
6
7
8
TIME, MINUTES OF MAGNETIC FIELD SWEEP

FIGURE 5

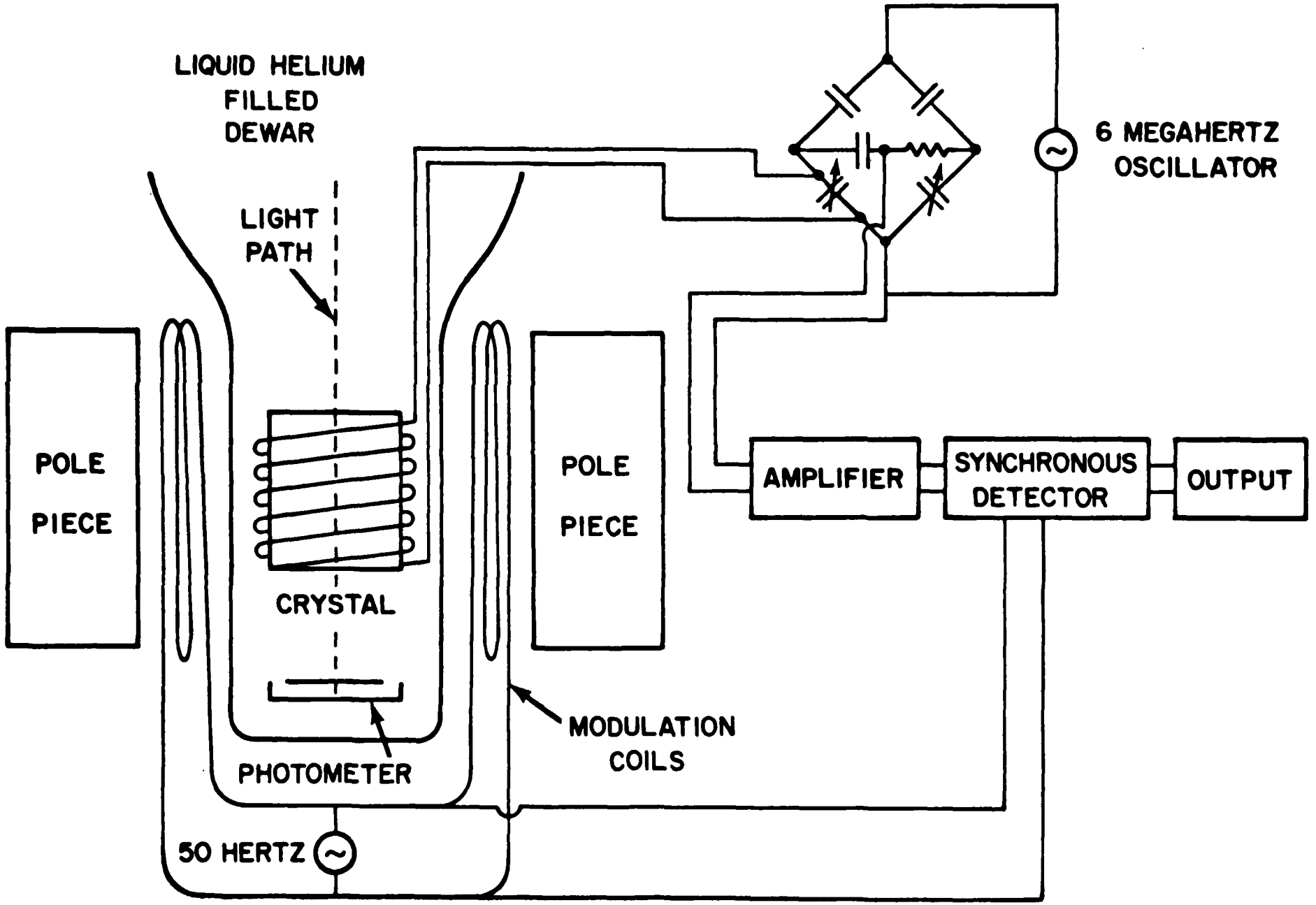
LIQUID HELIUM
FILLED
DEWAR
LIGHT
PATH
6 MEGAHERTZ
OSCILLATOR
POLE
PIECE
POLE
PIECE
AMPLIFIER
SYNCHRONOUS
DETECTOR
OUTPUT
CRYSTAL
MODULATION
COILS
PHOTOMETER
50 HERTZ

FIGURE 6

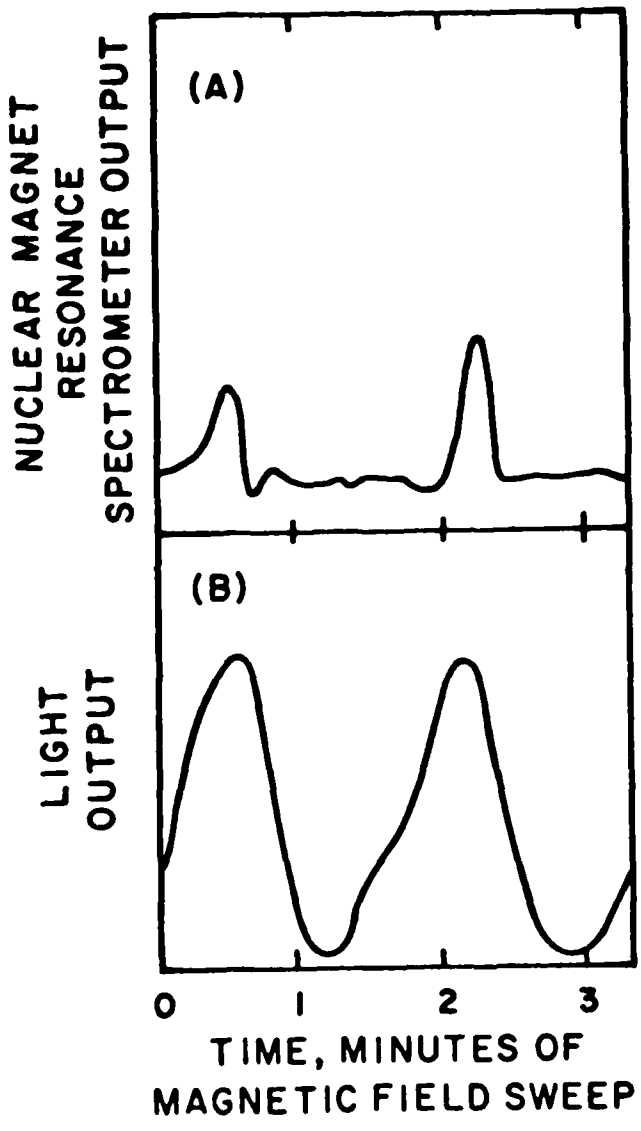
NUCLEAR MAGNET RESONANCE SPECTROMETER OUTPUT
(A)
(B)
LIGHT OUTPUT
0
1
2
3
TIME, MINUTES OF MAGNETIC FIELD SWEEP

FIGURE 7

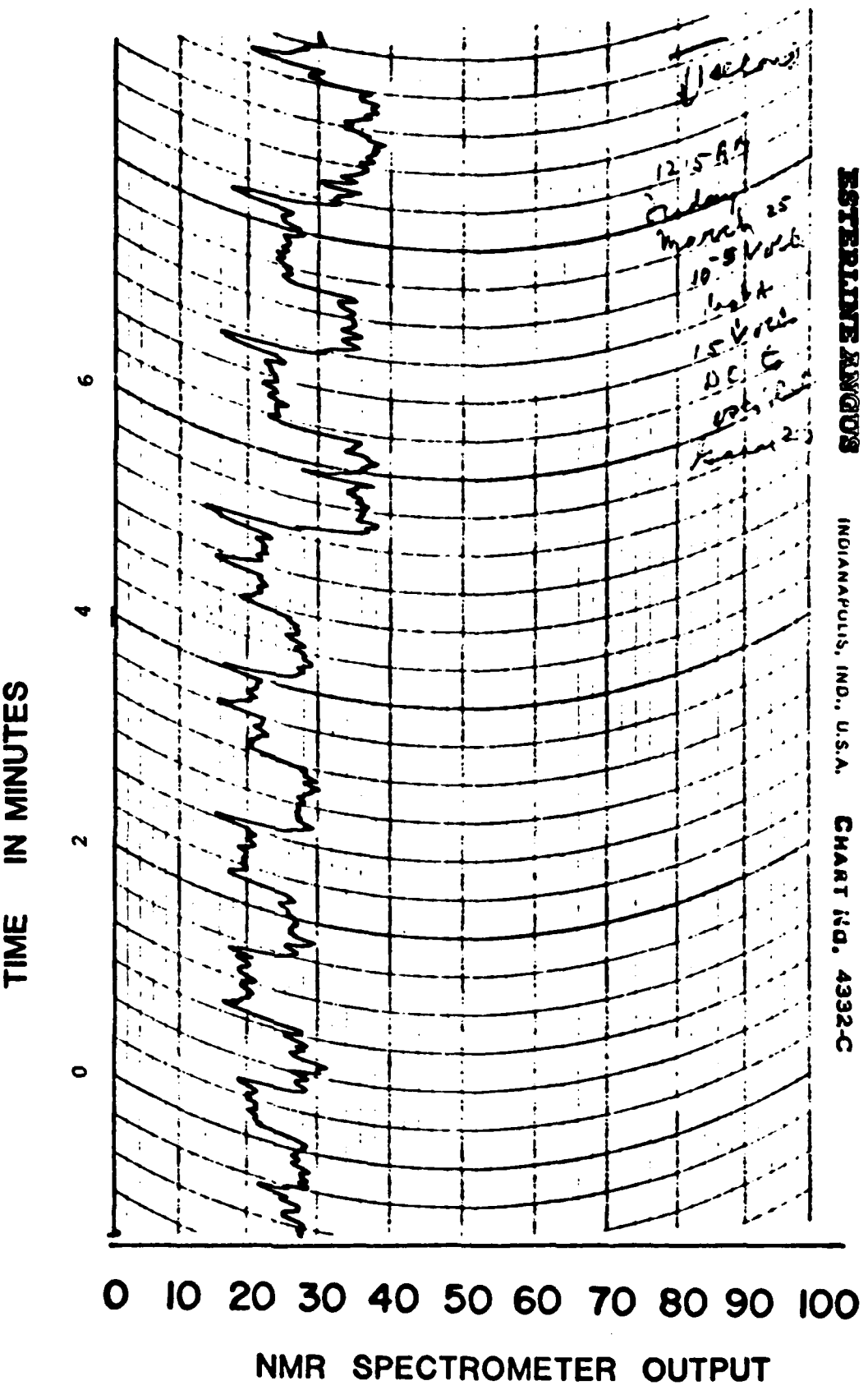
TIME IN MINUTES
0
2
4
6
0 10 20 30 40 50 60 70 80 90 100
NMR SPECTROMETER OUTPUT
ESTERLINE ANGUS
INDIANAPOLIS, IND., U.S.A.
CHART No. 4332-C

FIGURE 8

was again an important factor in the magnitudes of the correlations. At certain times there were nuclear spin slow heating effects (as interpreted from the NMR line heights) when the light was turned on. A thermistor mounted on the crystal indicated that the surface temperature of the crystal was unaffected by the light.

DISCUSSION OF THE EXPERIMENTS

The light output oscillations shown in Figures 2, 3, and 4 are believed to be caused by the Laser itself. Experiments have shown that an "unpolarized" Helium Neon Laser has linearly polarized light output with slowly variable polarization direction. The time scale of the polarization variations is similar to the time scale of the intensity oscillations of Figures 2, 3, and 4.

As a further check, experiments were carried out with a polarized Helium Neon Laser, in 1983, and confirmed during the period of the present grant. Again, approximately 10^{-12} watts of 632.8 nm light reached the photometer with zero applied magnetic field. A lens diffused the light so that the entire crystal cross section was illuminated.

Experiments were started in zero magnetic field, at 4.2 Kelvin. A magnetic field of 8000 Gauss was applied. This immediately reduced the intensity of the light measured by the photometer by about a factor 2. Then on a time scale of hours the intensity decreased, as shown by Figures 9, 11. When the magnetic field was reduced to a value approaching zero, the intensity increased as shown in Figure 10.

After several days at 4 K the spin system is very cold and the spin lattice coupling is relatively weak. Under these conditions the spins act as though they are isolated, with response to a radiofrequency field given by (40A'. (49) implies that the correlations $\langle a^*_{1s} a_{2s} \rangle$, and $\langle a_{1s} a^*_{2s} \rangle$ may contribute large changes to the total cross section.

ACKNOWLEDGEMENT

This research was supported in part by the Air Force Office of Scientific Research under Grant AFOSR-82-0164 and in part by the Advanced Research Projects agency monitored by the Air Force Office of Scientific Research under Contract F-49620-81C-0024.

CONCLUSION

Large cross sections predicted by theory for tightly coupled nuclei interacting with radiation, are observed for antineutrino scattering and coherent absorption of 632.8 nm red light.

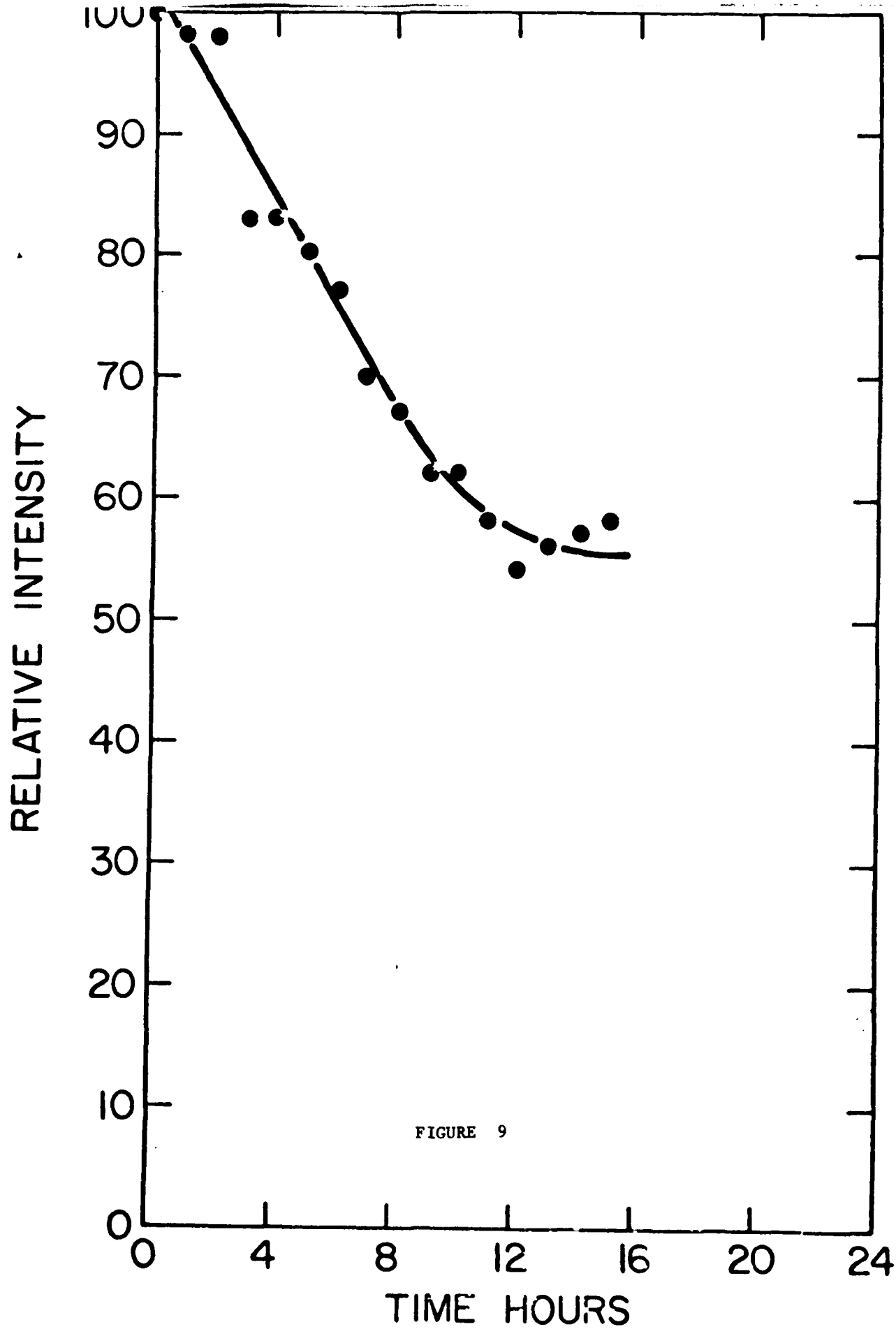
RELATIVE INTENSITY
100
90
80
70
60
50
40
30
20
10
0
0
4
8
12
16
20
24
TIME HOURS

FIGURE 9

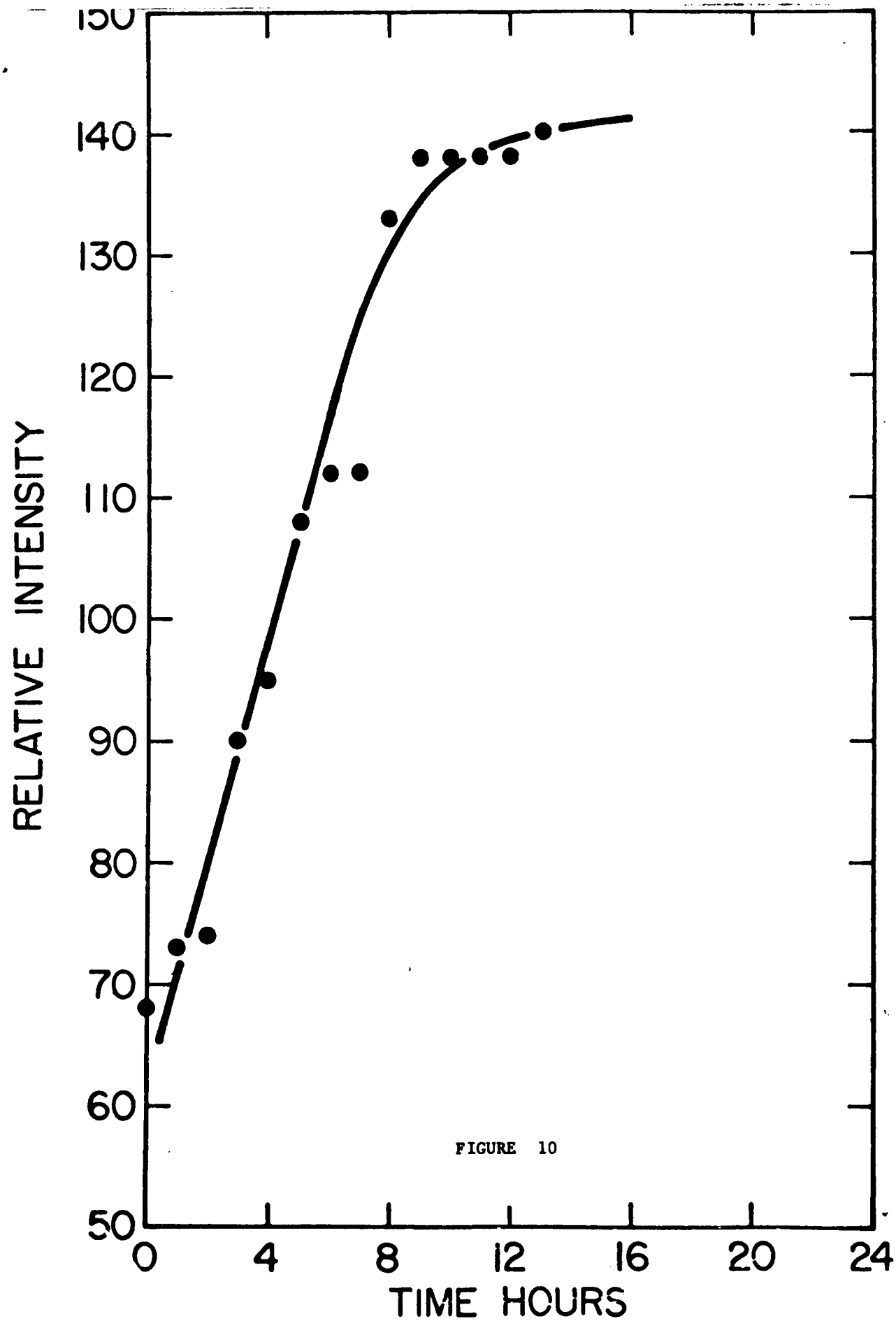
150
140
130
120
110
100
90
80
70
60
50
RELATIVE INTENSITY
0
4
8
12
16
20
24
TIME HOURS

FIGURE 10

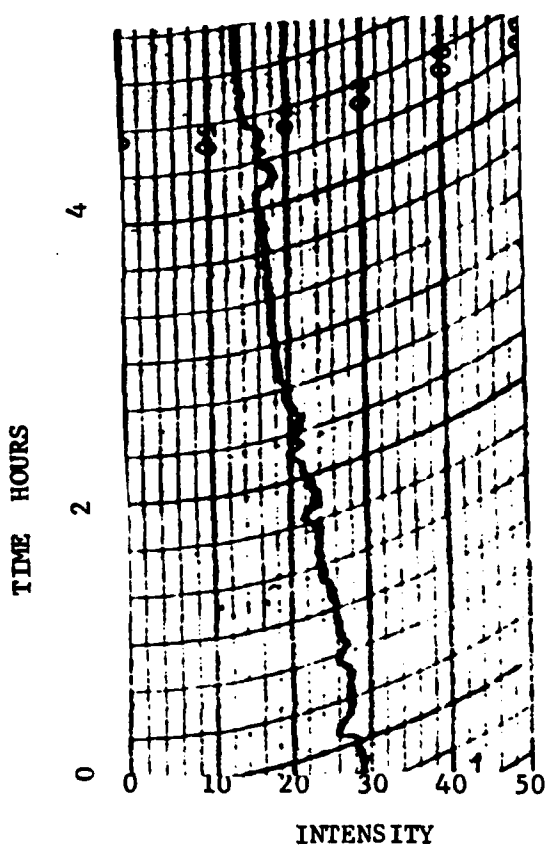

FIGURE 11 1986 DATA

FIGURE CAPTIONS

Figure 1 Interaction of Laser Light with a Crystal

Figure 2 Intensity of Transmitted Light Versus Time After Cooldown and Application of 8000 Gauss Magnetic Field for Lithium Flouride Crystals

Figure 3 Intensity of Transmitted Light Versus Time After Removal of 8000 Gauss Magnetic Field

Figure 4 Intensity of Transmitted Light Versus Time After Cooldown and Application of 8000 Gauss Magnetic Field for Sapphire Crystal

Figure 5 Correlation of Transmitted Light with Nuclear Magnetic Resonance Sweep

Figure 6 Nuclear Magnetic Resonance Spectrometer

Figure 7 Correlation of Transmitted Light with Nuclear Magnetic Resonance Sweep, *Averaging over Six Complete Cycles*

Figure 8 Correlations of Nuclear Magnetic Resonance Absorption with Incident Light

Figure 9 Intensity of Transmitted Light Versus Time After Cooldown and Application of 8000 Guass Magmetic Field to Sapphire Crystal, Light Source is a Polarized Helium Neon Laser

Figure 10 Intensity of Transmitted Light Versus Time After Removal of 8000 Gauss Magnetic Field, Light Source is a Polarized Helium Neon Laser

Figure 11 Intensity of Transmitted Light Versus Time After Cooldown and Application of 8000 Guass Magnetic Field to Sapphire Crystal, Light Source is a Polarized Helium Neon Laser

1.J.Weber, Phys. Rev. A.,23, 2, 761, 1981

2.Relativistic Quantum Theory Part 2 Chapter XV E. M. Lifshitz and L. P. Pitaevski 1974, Pergamon Press Ltd., Particle Physics, An Introduction, Chapter VI, M. Leon, Academic Press, 1973

3.Quantum Mechanics Non Relativistic Theory, Landau and Lifshitz, Volume 3, page 215

4.Relativistic Quantum Theory Part 1, page 214 V. B. Berestetskii, E. M. Lifshitz, and L. P. Pitaevski, 1971, Pergamon Press Ltd.

END

11-86

DTIC